FEBS Letters 354 (1994) 135–139

FEBS 14708

Disparate contributions of Tyr[10] and Tyr[109] to fluorescence intensity of rabbit skeletal muscle troponin C identified using a genetically engineered mutant

David Keleti, Venu G. Rao, Hong Su, Arvind B. Akella, Xiao-Ling Ding, Jagdish Gulati*

Molecular Physiology Laboratory, Division of Cardiology, Departments of Medicine and Physiology/Biophysics, Albert Einstein College of Medicine, Bronx, NY 10461, USA

Received 15 August 1994; revised version received 26 September 1994

Abstract Intrinsic tyrosines, as monitored by fluorescence spectroscopy, are sensitive reporters of local, Ca^{2+}-induced conformational changes in troponin C (TnC). Rabbit skeletal TnC contains two tyrosines (Y10 in the N-helix, and Y109 in site 3 in the C-terminal domain) in distinct microenvironments: their individual contributions to total fluorescence intensity are elucidated here utilizing bacterially synthesized rabbit skeletal TnC (sTnC4) and a genetically engineered variant, termed 109YF, lacking one of the tyrosines (Y109 replaced with F109). The steady-state fluorescence emission spectra following excitation at 280 nm were recorded in EGTA (Ca^{2+}-free) and Ca^{2+}-saturated (pCa4) solutions. For the wild-type sTnC4, pCa4 causes a significant (46%) increase in the peak fluorescence intensity over the value in EGTA. For the mutant 109YF, the EGTA fluorescence is only marginally affected (74% of the wild-type F_{EGTA}), but interestingly the Ca^{2+} effect is completely suppressed ($\Delta F = F_{pCa4} - F_{EGTA} = 2\%$ of the wild-type value). These results indicate that the two tyrosines make disparate contributions to the fluorescence spectrum of wild-type sTnC, both in the presence and absence of Ca^{2+}; whereas Y10 in the N-helix is dominant in Ca^{2+}-free solution, Y109 is the sole contributor to the Ca^{2+} effect. Furthermore, to explain the biphasic fluorescence response of Y109 obtained during Ca^{2+} titrations, the findings yield the most unequivocal evidence that Ca^{2+}-induced conformational changes in the trigger sites operating the contractile switch modify properties of the C-terminal sites in TnC pari passu.

Key words: Troponin; Calcium; EF hand structure; Muscle; Mutagenesis; Fluorescence

1. Introduction

Troponin C is the Ca^{2+}-binding component of the thin filament with a regulatory role in muscle contraction. The Ca^{2+}-induced conformational changes in the TnC molecule are transmitted across other regulatory components of the troponin complex, initiating the cross-bridge interactions between thick and thin filaments to switch on muscle contraction [1]. Therefore, many studies of Ca^{2+}-induced TnC conformations have been made recently to develop insights into the mechanism of the Ca^{2+}-switch for contraction (see [2,3]).

The fast-twitch skeletal muscle sTnC embodies four EF-hands for Ca^{2+}-binding [4]. Two Ca^{2+}-binding sites (sites 1 and 2) are in the N-terminal half and the other two (sites 3 and 4) are in the C-terminal half. These domains, joined in the crystal structure by a long central helix, have well-defined functions (N domain, trigger function; C domain, anchoring function) [1]. Another interesting feature of TnC is an N-helix preceding site 1, which too was the subject of several recent studies [5–8]. But the contractile function of the central helix remains unknown.

A useful biophysical approach to delineate Ca^{2+}-induced conformational changes in TnC is to examine the steady-state fluorescence emission by the intrinsic tyrosines. The rabbit skeletal TnC often used has two tyrosines – Y10 is in the N-helix, and Y109 resides within the Ca^{2+}-binding loop of site 3 – and the analyses of steady-state fluorescence emissions have yielded useful estimates for the affinity constants of the two classes of Ca^{2+}-binding sites in sTnC (i.e. the Ca^{2+}-specific regulatory low affinity sites and the Ca^{2+}/Mg^{2+} high affinity sites) [9–11]. Intrinsic tyrosines have more recently also been applied to time-resolved anisotropic decay studies where resonance energy transfer between the two tyrosines provided evidence for a model of a flexible central helix in sTnC [12,13], which has implications for possible interchange between the N- and C-terminal domains in the operation of the contractile Ca^{2+} switch. Yet, questions remained because the individual contributions of the two tyrosines in holo-TnC were never firmly delineated. The analysis of the Y10 and Y109 contributions to Ca^{2+}-dependent fluorescence is the major aim of this investigation.

To manifest these fluorescence properties of Y10 and Y109, the present study employs mutagenesis of rabbit sTnC cDNA to replace Y109 with F109, and compares the response of the resultant bacterially synthesized product with wild-type sTnC4. (The notation sTnC4 is used for wild-type fast-twitch skeletal muscle TnC to distinguish from unmodified tissue sTnC.) We find that Y10 and Y109 in sTnC4 confer disparate contributions to fluorescence intensities and respond variably to Ca^{2+} stimulation. The findings also provide further insights into the Ca^{2+} switch.

2. Materials and methods

2.1. TnC mutagenesis by genetic engineering

The modified protein was created by polymerase chain reaction (PCR) of the synthetic gene coding for rabbit sTnC that was cloned into a pT7 plasmid as previously described [14]. A linear representation of bacterially synthesized sTnC4 and the mutant generated is shown in Fig. 1. The two tyrosines (Y10 and Y109) of wild-type sTnC are marked. The Y10 is positioned at the terminal end of the putative N-helix and Y109 is a Ca^{2+}-coordinating residue within site 3.

The construct generated especially for the study here has a point mutation converting Y to F at position 109 (109YF mutant). Mutagenesis was directed in a PCR sequence by a 51 bp oligonucleotide containing the mismatches TAT→TTC, and another 3′ oligonucleotide

*Corresponding author. Fax: (1) (718) 823-0032.

SSDI 0014-5793(94)01095-1

downstream of the TnC-encoding region. The PCR product was subsequently cut with *Nhe*I and *Sac*I and inserted into the pT7-sTnC plasmid cut with the same enzymes.

2.2. Protein purification

The bacterially synthesized proteins were isolated and purified using a two-step purification procedure previously described [14]. Protein purity and characteristic Ca^{2+}-dependent mobilities were verified on 15% acrylamide gels as previously described [14]: both the mutant and the bacterial wild-type TnC exhibited the characteristic Ca^{2+}-induced mobility shift. Protein concentrations were measured by the Bio-Rad Protein Assay using an sTnC standard as previously described [14].

2.3. Ca^{2+} binding assay

The measurements were conducted with microdialysis on isolated proteins in a Ca^{2+}-saturated reservoir solution containing 100 μCi of $^{45}Ca^{2+}$ as described previously [5]. The amount of bound Ca^{2+} was estimated from the differential activity of the protein samples and reservoir solution, and the specific activity of the $^{45}Ca^{2+}$ added.

2.4. Permeabilized skinned fibers: TnC extraction and reconstitution

The muscle fiber single segments (typically 50 to 150 μm wide, and 2–4 mm long) were isolated from rabbit psoas fast-twitch muscle and permeabilized as before [15,16]. The relaxing and activating solutions modified from Gulati and Podolsky [17] were also as before [16–18]. The fiber was attached at both ends to the transducers, taking care to maintain the fiber length between the attachments at less than 4 mm for uniform activation. The sarcomere length following attachment was adjusted at 2.5 μm in the relaxing solution.

The TnC extractions and reconstitutions were generally the same as before [16,18]. The fiber was activated in pCa4 to record maximal force P_o before and after TnC manipulations. Care was also taken to ensure that the TnC reconstitution was complete.

For activations with submaximal Ca^{2+} concentrations, the techniques were as before [16,18]. The pCa–force relationships so determined were fitted by the Hill equation and the pCa_{50} values were computed as half-maximal activations by the least-squares fit. The Hill coefficients (n_H) were also derived.

2.5. Fluorescence spectroscopy

Spectroscopic measurements were conducted on a Shimadzu RF 5000U spectrofluorophotometer equipped with a temperature-controlled cuvette holder and a miniature magnetic stirrer [19]. The experimental temperature was maintained at 25°C. The excitation wavelength was set at 280 nm, and fluorescence intensities were monitored (in the presence and absence of Ca^{2+}) in the range of 290–340 nm. Ca^{2+} contamination present in the fluorescence buffer (0.1 M KCl, 0.1 M HEPES, pH 7.5, 2 mM EGTA) before titration was removed by passing the solution twice through Chelex-100 columns (Bio-Rad). In addition, all buffers and protein–buffer solutions were syringe-filtered through a 0.2 μm Acrodisc (Gelman Sciences) prior to fluorescence measurements. The Ca^{2+}-titrations were made as previously described [19]. The amounts of $CaCl_2$ required for Ca^{2+} titrations in a 2 mM EGTA solution were computed using association constants for Ca^{2+}-EGTA from Martell and Smith [20]. The pH 7.5 was maintained after each addition of $CaCl_2$. The titration data were fitted to the Hill equation and the apparent Ca^{2+} dissociation constant (pCa_{50}) and Hill coefficient value (n_H) were computed assuming two independent classes of Ca^{2+}-binding sites [26], and the final fit was obtained using SigmaPlot 5.0 (Jandel Scientific). Data for varying protein concentrations are expressed as mean ± S.E.M., with the best fit derived also with SigmaPlot 5.0 software.

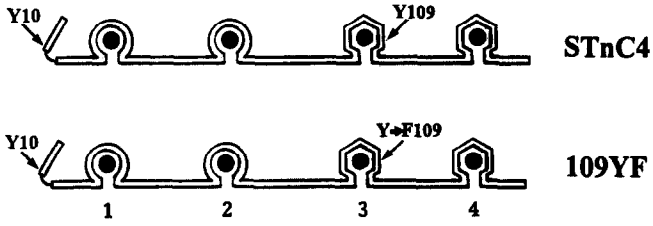

Fig. 1. A linear representation of sTnC4 and the mutant 109YF. The Ca^{2+}-specific low affinity sites (sites 1 and 2) are distinguished from the Ca^{2+}/Mg^{2+} high affinity sites (sites 3 and 4). Also marked are Y10 near the linker in the N-helix overhang, and Y109 in high affinity site 3.

3. Results

The aim of this study was to ascertain the individual contributions of rabbit sTnC Y10 and Y109 to the fluorescence emission spectra in EGTA and Ca^{2+}-saturated milieus. Since Y10 in the N-helix is located near the linker region, and Y109 resides within the loop of the Ca^{2+}/Mg^{2+} high affinity site in the C-terminal half of the molecule [4], the fluorescence spectra were expected to provide information regarding the roles of the N- and C-domains in the mechanism of the contraction switch. To meet the stated goal, we produced a mutant in which Y109 was replaced with F109, so that Y10 was left as the only fluorophore in the molecule. The fluorescence spectra of the mutant were determined in both EGTA and Ca^{2+}-saturated solutions and compared with corresponding measurements on wild-type sTnC4.

3.1. Ca^{2+}-binding capability and the skinned fiber properties of the mutant 109YF

For an assessment of the overall conformation of the mutant, the Ca^{2+}-binding capacities of tissue sTnC and wild-type sTnC4 were compared with the related capability of the mutant. These values were found to be similar for the three proteins. The summary results are listed in Table 1. The identity of the values suggests that the mutant retains its native configuration. Similarly, in isolated skinned fast-twitch skeletal muscle fibers (rabbit psoas) in which the endogenous sTnC was extracted and replaced with the mutant, the force characteristics (the maximal

Table 1
Functional characterization of the 109YF construct

	Purified protein data	Skinned fiber data		
	Ca^{2+}-bound (mol/mol)	Ca-activated force (% P_o)[a]	pCa_{50}[b]	n_H[c]
Native fiber	3.8 ± 0.1[d] (7)	100 (6)	5.74 ± 0.03 (5)	3.6 ± 0.1 (5)
sTnC4	3.9 ± 0.1 (19)	91 ± 1 (3)	5.75 ± 0.03 (3)	3.4 ± 0.1 (3)
109YF	4.0 ± 0.1 (11)	90 ± 2 (3)	5.71 ± 0.02 (3)	3.5 ± 0.2 (3)

Numbers in parentheses indicate the number of measurements.
[a] P_o is the pCa4-activated force on the skinned fiber. All values are normalized to the native (unextracted) fiber.
[b] The pCa_{50} represents the pCa value required for half-maximal activation according to the pCa–force relationship.
[c] n_H (Hill coefficient) represents the slope at the midpoint of the pCa–force relation.
[d] This value is for isolated tissue sTnC.

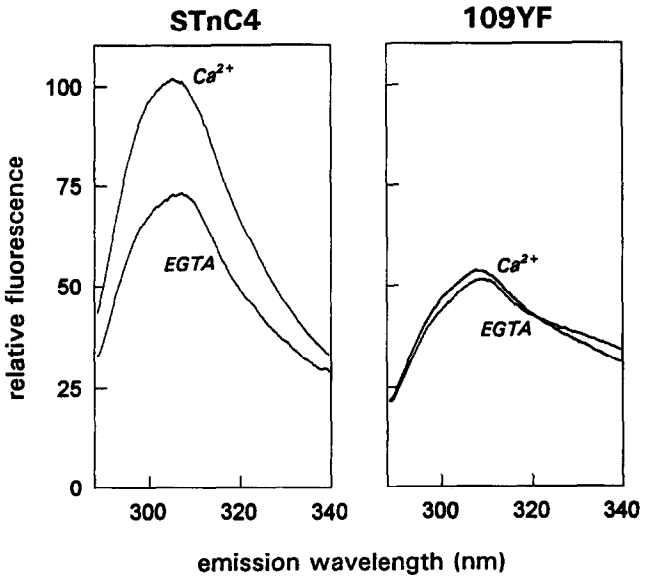

Fig. 2. Typical emission spectra of wild-type sTnC4 and 109YF (0.075 mg/ml). The spectra were recorded both in EGTA in the absence of Ca^{2+} (pCa > 9) as well as in the presence of 10^{-4} M Ca^{2+} (pCa 4).

force P_o, as well as pCa_{50} and the Hill coefficient n_H derived from the pCa–force relationships) were normal (Table 1). This is further evidence that the mutant 109YF retains the standard overall structure. Accordingly, we proceeded to study the fluorescence properties of this mutant.

3.2. Tyrosine fluorescence emissions in apo- and Ca^{2+}-saturated states

The characteristic emission spectra of 0.075 mg/ml wild-type sTnC4 in the presence of EGTA (pCa > 9) and after addition of saturating amounts of Ca^{2+} (pCa4) are shown in the left panel of Fig. 2. The excitation wavelength (λ_{exc}) was 280 nm and the peak emission wavelength (λ_{em}) is observed as 308 nm in EGTA and 306 nm in pCa4. The emission waveform in each case was normalized to the peak value for the wild-type in pCa4, which is depicted as 100. The addition of Ca^{2+} to wild-type sTnC4 induced a 46% enhancement in the intrinsic tyrosine fluorescence from that observed in the absence of Ca^{2+}.

The emission spectra of 0.075 mg/ml mutant (called 109YF) containing a single tyrosine are shown in the right panel of Fig. 2 (normalized to the pCa4 peak in the left panel). The peak intensity in EGTA is lower than the corresponding value for wild-type, although the peak emission wavelength λ_{em} in EGTA is 308 nm, the same as sTnC4. Also, the emission wavelength λ_{em} for the mutant in pCa4 is blue-shifted to 306 nm as it was for the wild-type protein. However, unlike the wild-type response in pCa4, the Ca^{2+}-induced emission intensity of the mutant is virtually unchanged from its value in EGTA. Increasing the free Ca^{2+} concentration to 1 mM elicited no additional response.

Normalized fluorescence intensities at peak emission wavelength of these proteins (wild-type sTnC4, and the 109YF mutant) at three concentrations in the presence and absence of Ca^{2+} are shown in Fig. 3. The normalized fluorescence intensities of these proteins, both in the presence and absence of Ca^{2+}, show a consistent linearity with increasing protein concentration.

A summary comparison of normalized fluorescence intensities (F_{EGTA}) of sTnC4 and the mutant (109YF) is shown in the upper panel in Fig. 4. In the absence of Ca^{2+}, the fluorescence intensities of the 109YF mutant with a single tyrosine Y10 (compared with two tyrosines in wild-type) are about 74% of the wild-type values at all protein concentrations, suggesting that the two tyrosines contribute unequally to the total EGTA fluorescence emission peak of rabbit sTnC. The mean of 4 measurements in each case indicated that Y10 accounts for 74 ± 3% of the total tyrosine fluorescence intensity observed in sTnC4, and by subtraction Y109 accounts for the remaining 26 ± 3%.

A similar comparison of the Ca^{2+}-induced fluorescence enhancement ($\Delta F = F_{pCa4} - F_{EGTA}$) of sTnC4 and the mutant is shown in the lower panel of Fig. 4. A negligible Ca^{2+}-induced enhancement is observed in the 109YF mutant ($\Delta F/F_{EGTA}$ = 2 ± 1%), suggesting that, despite its dominance in the determination of the F_{EGTA} value, Y10 contributes insignificantly to the Ca^{2+}-induced response. This is the most direct evidence to date that Y109 contributes to the bulk (98 ± 2%) of the Ca^{2+}-induced fluorescence enhancement seen in wild-type sTnC.

Interestingly, previous studies on tissue sTnC fragments [21], while indicating nearly identical quantum yields between Y10 (N-terminal fragment, residues 9–84) and Y109 (C-terminal fragment, residues 89–159) in EGTA, nevertheless showed consistently with our present results on intact sTnC4 that only the fragment with Y109 gave a Ca^{2+}-induced fluorescence enhancement. On the other hand, the high F_{EGTA} of the Y109 fragment is inconsistent with the fluorescence response of holo-sTnC4 and reflects the modified structure of the C-terminal fragment.

3.3. Ca^{2+} titrations of Tyr^{109} fluorescence emission

The typical fluorescence Ca^{2+} titrations of recombinant sTnC4 are shown in Fig. 5. The biphasic nature of this curve was evident, with the first transition representing 70% and the second representing 30% of the total fluorescence response. The corresponding pCa_{50} values (Table 2) are 7.13 and 6.42, representing the Ca^{2+}/Mg^{2+} high affinity sites and the Ca^{2+}-specific low affinity sites respectively. These values are also similar to those found by Grabarek et al. using extrinsic probes [22]. The Hill coefficients indicated in Table 2 are indistinguishable between the high affinity and low affinity sites.

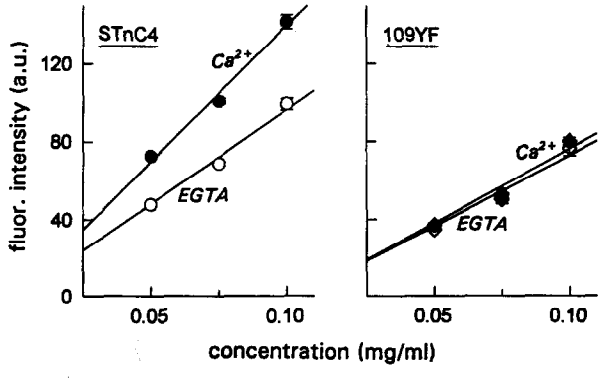

Fig. 3. The dependence of fluorescence intensity upon protein concentration in the presence and absence of Ca^{2+}.

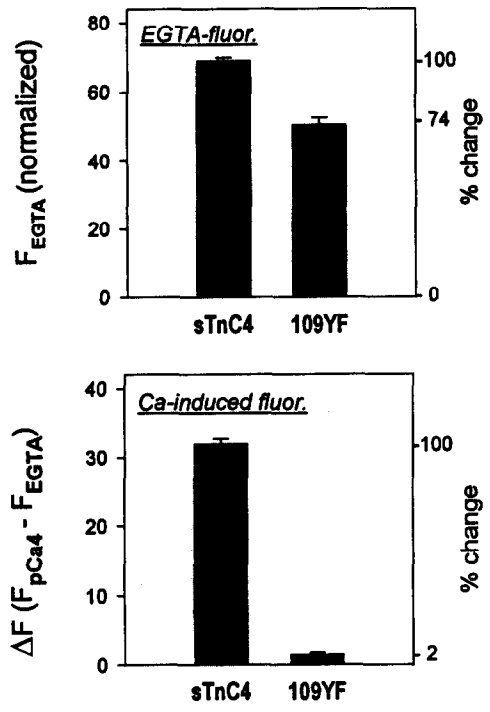

Fig. 4. Summary of fluorescence intensities F_{EGTA} (upper panel) and ΔF (lower panel) of sTnC4 and the mutant 109YF at 0.075 mg/ml concentrations. Normalized values are indicated by the scale on the right hand side.

4. Discussion

With bacterially synthesized rabbit skeletal troponin C and a genetic variant, we have been able to quantitate the disparate contributions of Y10 and Y109 to fluorescence intensity in the presence and absence of Ca^{2+}. Under native conditions, Y10 is found to contribute 74% of the F_{EGTA}, but only a negligible amount of the ΔF (i.e. $F_{pCa4} - F_{EGTA}$) observed in sTnC. Conversely, Y109 contributes the remaining 26% of the F_{EGTA} but accounts for the bulk of the ΔF observed in sTnC4. The disparate contributions tyrosines Y10 and Y109 to the emission spectrum of the protein are explained by the dissimilar microenvironments of the two tyrosines. For instance, Y109 is intimately involved in hydrogen bondings with the nearby carboxylates of D103 and D107 [23], and thereby experiences significant collisional quenching in EGTA. On the other hand, the crystal structure reveals no H-bondings for Y10. Indeed, the hydrogen bonded phenols are generally non-fluorescent or minimally fluorescent [24]. Since D103 and D107 as well as Y109 are also the key coordinates for Ca^{2+}-binding in site 3, the sizable Ca^{2+}-induced fluorescence enhancement generated by Y109 is then explained by the expected release of the constraints due to shifts in the carboxylates from hydrogen bonding towards the coordination of the Ca^{2+} ion [25].

Table 2
Fluorescence parameters for biphasic pCa titrations

	High affinity sites	Low affinity sites
pCa_{50}	7.13 ± 0.08	6.42 ± 0.05
n_H	2.23 ± 0.3	1.90 ± 0.4
% F	69 ± 1	31 ± 1

The pCa_{50} represent the pCa values derived for the individual sets of sites from half-maximal change in % fluorescence, n_H are the Hill coefficient values, and % F are the percentages of total change in fluorescence. The data are mean ± S.E.M. of four experiments.

4.1. Implications for the interactions between the N- and C-domains of TnC

The significance of our findings for the possible interactions between the two classes of Ca^{2+}-binding sites should also be considered. The fluorescence response obtained during Ca^{2+} titration of bacterially expressed sTnC4 is composed of two distinct phases (Fig. 5); a high affinity phase accounting for about 70% of the tyrosine fluorescence enhancement, and a low affinity phase accounting for the remaining 30%. A similar biphasic response was also observed on tissue sTnC [9,11]. Moreover, in light of the finding that Y109 accounts for virtually all of the Ca^{2+}-induced response, the evident implication is that the entire biphasic response must be generated from the same fluorophore. We thereby conclude that Ca^{2+} binding to the low affinity sites of sTnC (occurring in the upper phase of the curve between pCa 6.7 and 5.0) induces a conformational change in the high affinity sites as monitored by Y109. This is then firm evidence that, despite the extended central helix connecting the N- and C-lobes of TnC, a conformational signal is communicated between the two classes of binding sites (see also [22,26]). However, whether this intramolecular communication is essential for the on–off function of the Ca-switch, and/or whether it modulates the regulation of contraction beyond the on–off step, remains to be ascertained.

A recent study by Babu et al. [16] provided information also pertaining to these questions. For instance, with a modified sTnC4 embodying a severely curtailed central helix, Babu et al. observed that two such molecules were present during the operation of the contractile switch [16]. This could indicate that the on–off switching was possible even when a single molecule was too short to perform both the triggering and anchoring functions simultaneously. On the other hand, it was possible in the Babu et al. study also that the two short molecules remained in intimate communication to execute the switching mechanism, which would suggest, moreover, that the information dialog could be effected over distances even longer than in a standard dumb-bell TnC. These ambiguities may be resolved in future studies with genetically engineered molecules sufficiently short to preclude the intermolecular contact.

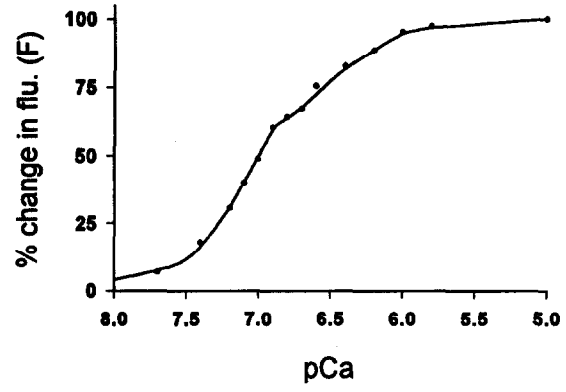

Fig. 5. The Ca^{2+}-dependent change in Tyr^{109} fluorescence of recombinant skeletal troponin C.

4.2. The Ca^{2+}-dependent disposition of the N-helix in sTnC

Recent studies have established the need for the N-helix in the contraction mechanism [5,7]. Thus, it was of interest that Ca^{2+} ions had little effect on the fluorescence signal emitted by Y10, suggesting that the microenvironment of this fluorophore is relatively stable. However, because of the proximity of the fluorophore to the linker region between the N-helix and site 1, the unresponsiveness of Y10 to Ca^{2+} is also the expected result if, in the activated state, the N-helix were to shift away from its resting position using the linker as the pivot (e.g. [8]). This and other possibilities should be examined in the future.

Acknowledgements: Grant support was from NIH (AR-33736), the New York Heart Association, and the Blumkin Fund.

References

[1] Zot, A.S. and Potter, J.D. (1987) Annu. Rev. Biophys. Chem. 16, 535–559.
[2] Grabarek, Z., Tao, T. and Gergely, J. (1992) J. Mus. Res. Cell Mot. 13, 383–393.
[3] Gulati, J., Babu, A., Cheng, R. and Su, H. (1993) in: Modulation of Cardiac Calcium Sensitivity (Lee, J.A. and Allen, D.G., eds) pp. 215–241, Oxford University Press, New York.
[4] Strynadka, M.N.J. and James, M.N.G. (1989) Annu. Rev. Biochem. 58, 951–998.
[5] Gulati, J., Babu, A., Su, H. and Zhang, Y.F. (1993) J. Biol. Chem. 268, 11685–11690.
[6] DaSilva, E.F., Sorenson, M., Smillie, L., Barrabin, H. and Scofono, H. (1993) J. Biol. Chem. 268, 26220–26225.
[7] Smith, L., Greenfield, N.J. and Hitchcock-DeGregori, S.E. (1994) J. Biol. Chem. 269, 9857–9863.
[8] Ding, X.-L., Akella, A.B., Su, H. and Gulati, J. (1994) Protein Sci. (in press).
[9] Johnson, J. and Potter, J. (1978) J. Biol. Chem. 253, 3775–3777.
[10] Wang, C.L., Leavis, P.C., Horrocks, W.D. and Gergely, J. (1981) Biochemistry 20, 2439–2444.
[11] Van Eyk, J.E., Kay, C.M. and Hodges, R.S. (1991) Biochemistry 30, 9974–9981.
[12] Wang, C.K., Liao, R. and Cheung, H.C. (1993) J. Biol. Chem. 268, 14671–14677.
[13] Wang, C.-L.A., Leavis, P.C. and Gergely, J. (1983) J. Biol. Chem. 258, 9175–9177.
[14] Babu, A., Su, H., Ryu, R. and Gulati, J. (1992) J. Biol. Chem. 267, 15469–15473.
[15] Gulati, J. (1976) Proc. Nat. Acad. Sci. USA 73, 4693–4897.
[16] Babu, A., Rao, V.G., Su, H. and Gulati, J. (1993) J. Biol. Chem. 268, 19232–19238.
[17] Gulati, J. and Podolsky, R.J. (1978) J. Gen. Physiol. 72, 701–716.
[18] Babu, A., Scordilis, S., Sonnenblick, E. and Gulati, J. (1987) J. Biol. Chem. 262, 5815–5822.
[19] Gulati, J. and Rao, V.G. (1994) Biochemistry 33, 9052–9056.
[20] Martell, A.E. and Smith, R.M. (1974) Critical Stability Constants, Plenum Press, New York.
[21] Leavis, P.C., Rosenfeld, S.S., Gergely, J., Grabarek, Z. and Drabokowski, W. (1978) J. Biol. Chem. 253, 5452–5459.
[22] Grabarek, Z., Leavis, P.C. and Gergely, J. (1986) J. Biol. Chem. 261, 608–613.
[23] Herzberg, O. and James, M.N.G. (1988) J. Mol. Biol. 203, 761–779.
[24] Lakowicz, J.R. (1983) Principles of Fluorescence Spectroscopy, Plenum Press, New York.
[25] Leavis, P.C. and Lehrer, S.S. (1978) Arch. Biochem. Biophys. 187, 243–251.
[26] Dobrowolski, Z., Xu, G.-Q. and Hitchcock, S.E. (1991) J. Biol. Chem. 266, 5703–5710.